The Journal of Experimental Biology 202, 2749–2761 (1999)
Printed in Great Britain © The Company of Biologists Limited 1999
JEB2379

THE DIVING PHYSIOLOGY OF BOTTLENOSE DOLPHINS (*TURSIOPS TRUNCATUS*)

II. BIOMECHANICS AND CHANGES IN BUOYANCY AT DEPTH

RANDOLPH C. SKROVAN[1], T. M. WILLIAMS[1,*], P. S. BERRY[2], P. W. MOORE[3] AND R. W. DAVIS[4]

[1]*Department of Biology, Earth and Marine Science Building, A-316, University of California, Santa Cruz, CA 95064, USA,* [2]*The Dolphin Experience, PO Box F42433, Freeport, Grand Bahama Island, Bahamas,* [3]*SPAWAR Systems Center, D35, 53560 Hull Street, San Diego, CA 92152-6506, USA* and [4]*Department of Marine Biology, Texas A&M University, Galveston, TX 77553, USA*

*Author for correspondence (e-mail: williams@darwin.ucsc.edu)

Accepted 26 July; published on WWW 30 September 1999

Summary

During diving, marine mammals must balance the conservation of limited oxygen reserves with the metabolic costs of swimming exercise. As a result, energetically efficient modes of locomotion provide an advantage during periods of submergence and will presumably increase in importance as the animals perform progressively longer dives. To determine the effect of a limited oxygen supply on locomotor performance, we compared the kinematics and behavior of swimming and diving bottlenose dolphins. Adult bottlenose dolphins (*Tursiops truncatus*) were trained to swim horizontally near the water surface or submerged at 5 m and to dive to depths ranging from 12 to 112 m. Swimming kinematics (preferred swimming mode, stroke frequency and duration of glides) were monitored using submersible video cameras (Sony Hi-8) held by SCUBA divers or attached to a pack on the dorsal fin of the animal. Drag and buoyant forces were calculated from patterns of deceleration for horizontally swimming and vertically diving animals. The results showed that dolphins used a variety of swimming gaits that correlated with acceleration. The percentage of time spent gliding during the descent phase of dives increased with depth. Glide distances ranged from 7.1±1.9 m for 16 m dives to 43.6±7.0 m (means ± S.E.M.) for 100 m dives. These gliding patterns were attributed to changes in buoyancy associated with lung compression at depth. By incorporating prolonged glide periods, the bottlenose dolphin realized a theoretical 10–21 % energetic savings in the cost of a 100 m dive in comparison with dives based on neutral buoyancy models. Thus, modifying locomotor patterns to account for physical changes with depth appears to be one mechanism that enables diving mammals with limited oxygen stores to extend the duration of a dive.

Key words: dolphin, *Tursiops truncatus*, diving, biomechanics, buoyancy.

Introduction

Animals demonstrate a wide variety of mechanical, morphological and behavioral adaptations that promote locomotor efficiency and subsequently reduce the overall cost of activity. Terrestrial animals systematically change gaits, moving from walk to trot to gallop as speed increases (Heglund et al., 1974; Taylor, 1978; Hoyt and Taylor, 1981; Magana et al., 1997). During walking, these animals conserve energy by alternately storing and releasing gravitational potential energy as they rotate over a stiffened limb. With the change to a gallop, bound or hop, elastic elements in the limbs and spine may be used to store and recover energy as the speed of a terrestrial animal increases (Taylor, 1978; Williams, 1983).

Similarly, aquatic vertebrates use a variety of strategies to reduce the cost of locomotion. Burst-and-glide swimming and schooling, observed in many species of fish, promote energy conservation (Fish et al., 1991). The low drag associated with gliding periods during interrupted forms of swimming appears to compensate for the increased effort of re-acceleration during burst phases (Blake, 1983). Schooling behavior also reduces the energetic cost for individuals moving in groups by decreasing the relative drag encountered by the trailing swimmers (Breder, 1965; Belyayev and Zuyev, 1969; Weihs, 1973; Abrahams and Colgan, 1985).

Locomotor efficiency is especially important for aquatic mammals during diving. When submerged, marine mammals must balance the energetic demands of exercise with the conservation of a limited oxygen store (Castellini, 1985; Castellini et al., 1985). High locomotor costs will presumably lead to the termination of a dive as oxygen reserves are quickly depleted. Conversely, locomotor efficiency may be manifest as an increase in time available at depth for locating and catching prey or for predator avoidance (Williams, 1996).

Most studies addressing locomotor performance in marine

mammals have focused on transit-swimming animals moving near the water surface (Fish, 1992). For example, the routine speeds (Lang and Norris, 1966; Lang, 1974; Würsig and Würsig, 1979; Williams et al., 1992), boundary flow characteristics (Rohr et al., 1998) and burst performances (Hui, 1987) of bottlenose dolphins have been reported. In comparison, there is little information concerning the underwater performance capabilities and limitations of these animals. In view of this, the present study examined the behavior and biomechanics of diving bottlenose dolphins (*Tursiops truncatus*) and the effect of a limited oxygen supply on underwater performance. Factors contributing to locomotor efficiency during submergence were investigated. To assess the relationships between swimming mode, stroke mechanics and dive depth, we videotaped dolphins during (1) horizontal swimming near the water surface, (2) horizontal swimming at depth, and (3) vertical diving to depths ranging from 12 to 112 m. Digital analyses of the video sequences were used to define locomotor modes and their pattern of use, glide duration and rates of acceleration and deceleration. These data, in combination with information from time/depth and velocity recorders, allowed changes in drag and buoyancy due to depth to be determined. The results of this study indicate that dolphins exploit changes in buoyancy associated with pressure changes at depth. By incorporating prolonged glide periods during descent, dolphins can reduce the period of active stroking and related energetic costs. Thus, glide performance by dolphins provides one important mechanism for conserving limited oxygen stores during submergence.

Materials and methods

Animals

Six trained Atlantic bottlenose dolphins (*Tursiops truncatus*) were used in this study (Table 1). All animals were housed in net pens (>15 m×15 m×4 m deep) connected to the open ocean. The dolphins were fed a diet of capelin and herring supplemented with multivitamins (Sea Tabs™, vitamin C, B-12 and B complex). Five of the animals were housed at the Dolphin Experience (Grand Bahama Island, Bahamas). Two adult male dolphins (B1, B2) and one adult female (B3) were used during uninstrumented dives to 12–14 m and for horizontal swims on the water surface and while submerged. A second female (B4) and an immature male (B5) were also used for surface swimming tests. Deep dives and horizontal submerged swims were performed by an adult male dolphin (S6) wearing an instrument package. This animal was housed at the U.S. Navy SPAWAR Systems Center (San Diego, California, USA).

Experimental design

The swimming mechanics and behavior of dolphins were examined under four conditions: (1) steady-state horizontal swimming near the water surface, (2) horizontal swimming at depths of 5–14 m, (3) shallow dives to 12 m without instrumentation on the dolphins, and (4) deep dives ranging from 16 to 112 m with the animal wearing an instrumentation package. Horizontal swimming, both near the surface and at depth, was used to evaluate the swimming mode of dolphins in the absence of changes in buoyancy. Deep dives of 16–112 m allowed a comparison of locomotor behaviors as buoyancy and demands on oxygen reserves changed with the depth and duration of the dive. Swimming and gliding performance of dolphins with and without instrumentation were also compared to determine the potential effects of the instrument package on the locomotor behavior and hydrodynamic drag of the animals.

Table 1. *Age and morphological dimensions of the bottlenose dolphins used in this study*

Animal	Age (years)	Length (cm)	Fluke span (cm)	Mass (kg)	Location
B1	13	249	64	236	Bahamas
B2	13	254	72	227	Bahamas
B3	13	237	68	173	Bahamas
B4	13	233	61	177	Bahamas
B5	2	188	N/A	82	Bahamas
S6	16	236	66	177	San Diego

Age was estimated from body length and duration in captivity.
Body length is the straight-line distance from the tip of the rostrum to the fluke notch.
N/A, not applicable.

Horizontal swimming

The kinematics of bottlenose dolphins swimming near the water surface was recorded using a hand-held video camera (Sony Hi-8, model CCD TR400). Dolphins were videotaped while swimming alongside a 17 foot Boston Whaler traveling at either 1.5 or 3.7 m s^{-1}. Boat speed was controlled by maintaining the outboard motor at constant revs min^{-1} with the same motor trim for all runs. Speed associated with each revs min^{-1} was determined by videotaping the boat's passage past fixed points a measured distance apart. Video sequences of the fixed points were digitized, and speed was determined using a motion-analysis system (Peak Performance Technologies, Inc.; Englewood, CO, USA). Trainers maintained the position of the dolphins abeam of the boat outside the stern and bow wakes. Analyses were limited to video segments in which the dolphins remained clear of interfering wakes and were stationary relative to the moving boat.

Horizontal swimming was also examined for submerged dolphins moving between two trainers at a depth of 14 m or between stationary targets at approximately 5 m depth. During the 14 m trials, movements of the dolphins were recorded by a SCUBA diver with a hand-held video camera in a submersible housing (Stingray, Inc.). The camera was held in a stationary position perpendicular to the swimming path of the animals. Progress across the field of view was converted to speed (m s^{-1}) using the motion-analysis system described above.

Images were digitized and calibrated against the measured length of the dolphin. To account for extraneous movements of the camera, a fixed point on the sea floor within the field of view was digitized using Peak Performance software (Englewood, CO, USA). Movement vectors of the fixed point were then subtracted from movement vectors of the dolphin. In addition to these trials, fluke movements of a dolphin swimming horizontally at approximately 5 m depth were recorded for an animal wearing a submersible video/instrument package (described below). Horizontal swim paths at depth ranged from 10 to 100 m in length.

Shallow dives

Straight-line dives to less than 16 m in depth were recorded in the Bahamas by a SCUBA diver using a hand-held video camera in a submersible housing (described above). On each experimental day, two dolphins followed a motor boat to an open ocean site 1 mile (1.61 km) offshore. Sites ranged from 12 to 16 m in depth with a sand bottom. Dolphins were trained to dive between the boat and a trainer stationed at depth. The animals chose their rates of ascent and descent, surface interval between dives and bottom time. Each session was recorded by a diver positioned perpendicular to the movements of the dolphins and as far back as visibility allowed. Depending on the distance from the subject, the field of view for the camera was 7–14 m. A field of view of 14 m allowed the entire ascent and descent of the dolphins to be monitored without panning the camera. When necessitated by surge, a monopod was used to stabilize the camera. To control for inadvertent camera movement, a stationary reference point was digitized, and its movement vector was subtracted from the dolphin's track. Measurements of fluke movement and velocities were not sensitive to camera range because each video sequence was calibrated against the measured length of the dolphin.

Deep dives

Fluke movements during deep (16–112 m) diving were recorded by a submersible video camera worn by the dolphin. A saddle platform containing the camera and instrumentation was custom-fitted to the dorsal fin of one dolphin, S6. The dolphin was trained for 6 weeks prior to the experiments to swim and dive while wearing the instrument package. This on-board system enabled us to examine the fluke movements of the dolphins at depths exceeding 100 m, which were outside the range of SCUBA divers.

The instrument package included a time/depth recorder, velocity meter, camera head (See-snake) surrounded by blue light-emitting diodes and video recorder. The camera head was directed backwards to record the stroke activity of the dolphin's fluke. Video sequences and dive variables were synchronized using custom-designed software (Pisces Design; San Diego, CA, USA). The instrument package and platform were neutrally buoyant and constructed of non-compressible materials to maintain neutrality at depth. The mass of the package was 14 kg, representing 8 % of the dolphin's mass. Because the package was neutrally buoyant, there was no additional weight for the dolphin to bear. However, its mass affected the acceleration of the dolphin. Details of the camera and instrument package are described by Davis et al. (1999).

The stall speed and accuracy of the velocity meter, as well as the accuracy of the time/depth recorder, were determined prior to deployment. The minimum recording (stall) speed of the velocity meter was measured by towing the instrument package attached to a fusiform shape through an annular water trough (Scripps Institute of Oceanography, La Jolla, CA, USA). In addition, the velocity meter was self-calibrated on the diving dolphin by plotting the velocity of the animal against the rate of depth change (S. Blackwell, personal communication). The latter method provides accurate calibration of the velocity meter if any portion of a dive is near vertical. Observations from the surface and video recordings indicate that this condition was met in the present study. The depth sensor was calibrated before and after the experimental period. The accuracy of the depth sensor was tested on a pressure station at 0–1500 psi (0–10.4 MPa) and was found to be linear over the test range (r^2=0.99) with a mean standard deviation of ±0.2 %. Depth and velocity were recorded at 1 s intervals throughout the dives.

Ten dives to 16 m were conducted inside San Diego Bay, CA, USA. During these trials, the dolphin followed a boat (Boston Whaler, 21 foot) to the dive site, where the instrument package was placed on the dolphin and secured using a strap. An acoustic pinger attached to a video camera was lowered to 16 m. The camera was cabled to a monitor on the boat and used to confirm the animal's arrival at depth. Following a signal from the trainer, the dolphin submerged to the pinger. On arrival, the acoustic signal was turned off and the animal returned immediately to the boat. A rest period of at least 1 min was provided between dives. The mean rest period was 46±23 s before the dolphin voluntarily began diving.

Eighteen dives of 50–112 m were conducted in the open ocean approximately 5 miles (8.1 km) off the coast of San Diego, CA, USA. To avoid fatigue during these deep diving tests, the dolphin was transported by boat to the dive site, where it was immediately returned to the water. The instrument package was placed on the dolphin, and the acoustic pinger was lowered to the test depth (50 or 100 m). Testing procedures were as described for 16 m dives. Recovery periods averaged 2.5 min between dives, during which the respiratory rate of the animal was monitored. Respiratory rate was determined by counting the number of breaths taken during the first minute immediately following the dive (Williams et al., 1999).

Analysis

The swimming mode and kinematics of uninstrumented dolphins were determined from video sequences from the hand-held camera using a motion-analysis system (Peak Performance Technologies, Inc.; Englewood, CO, USA). Each swimming or diving segment was converted to digital format. Anatomical points of interest (for details, see Fig. 1A) were manually digitized for 1–60 images per second of video recording. The acceleration, deceleration, angular acceleration

and speed of each point were then computed. In addition, stroke amplitude and the distance traveled by the dolphins while stroking or gliding were assessed for each video sequence. Changes in the amplitude (as a proportion of total body length) of the anatomical points were calibrated against the measured length of each dolphin.

Video images from the instrument package worn by the dolphin on deep dives were copied onto VHS tapes with data overlay from the time/depth recorder and velocity meter. The annotated video recording was analyzed 'frame by frame' for patterns in swimming mode and type of stroke. Strokes were categorized as large, medium, small or gliding according to the arc swept by the fluke. Stroke type was correlated to changes in depth, speed and acceleration of the dolphin.

Drag and buoyant forces were determined from videotaped sequences of horizontally swimming or vertically diving dolphins, respectively. Total body drag was calculated by multiplying the measured rate of deceleration of horizontally gliding dolphins by the total mass decelerated. Deceleration was determined from the change in speed at 1 s intervals and averaged over the glide period. The mass of dolphin S6 was 177 kg, and the mass of the instrument package was 14 kg. Because accelerating a body within a fluid also involves accelerating the surrounding fluid (Daniel, 1984; Lovvorn et al., 1991; Vogel, 1981), we accounted for the mass of the entrained water moving with the dolphin. This is equivalent to the mass of water displaced by the animal multiplied by the coefficient of added mass (0.06 for a prolate spheroid of fineness ratio 5.0; Vogel, 1981). On the basis of this calculation, the mass of the entrained water was 11 kg, and the total mass of the instrumented animal moving through the water was 202 kg. It is likely that the coefficient of added mass used in these calculations is conservative for a dolphin-shaped body and that the actual added mass may be greater because of water entrained by body contours or fins. Calculations based on a less-streamlined shape (i.e. a fineness ratio of 4.0) result in only a 2.1 % increase in the predicted total mass of the instrumented animal. Such a difference would not significantly alter our calculations for body drag and buoyant force.

Buoyancy in diving dolphins was calculated from the differences in deceleration between vertical and horizontal glides. The changes in buoyancy were ascribed to changes in volume with depth due to the compression of air spaces by water pressure. For dolphins, the lungs represent an important, compressible air space. Air in the lungs imparts a buoyant force equal to the amount of water displaced according to Archimedes' principle (Giancoli, 1984). During diving, pressure increases by 1 atm (98.1 kPa) for every 10 m increase in depth (Heine, 1995). Because volume varies inversely with pressure, the lung volume of the dolphins will decrease with depth. On the basis of these principles, the change in air volume of the lungs is described by:

$$V_D = V_S/(1 + 0.1h)\,, \quad (1)$$

where V_D is air volume in liters at depth, V_S is the air volume in liters at the surface, and h is depth in meters. The buoyant force at any depth can be determined for the dolphin from lung volume added to the buoyant force of its body. The resulting equation is:

$$B_D = V_D\boldsymbol{g} + B_B\,, \quad (2)$$

where B_D is the buoyant force in newtons at depth, V_D is the air volume in liters at depth from equation 1, $\boldsymbol{g}$ represents the acceleration due to gravity (9.8 m s^{-2}) and B_B is buoyancy in newtons of the dolphin's body without air (–33.2 N for dolphin S6; see equation 7). Note that the air volume in liters is equivalent to the mass of the displaced water in kilograms. During vertical glide sequences, upward buoyant forces oppose the downward pull of gravity. The resultant force will hereafter be referred to as a positive buoyant force when the net force is upwards and as a negative buoyant force when the net force is downwards.

Effects of instrumentation on dolphin performance

Previous studies indicate that the addition of recording instruments may alter the performance of an aquatic animal by increasing drag and by adding inertial mass (Wilson et al., 1986; Boyd et al., 1997). The total frontal area of the instrument package in the present study represented approximately 22 % of the dolphin's frontal area. The instruments were evenly divided between each side of the dolphin, with the front end of the instruments being tapered to minimize drag. We determined the changes in total body drag of the dolphins due to the instrument package by comparing horizontal glide deceleration for instrumented and uninstrumented animals. Behavioral and mechanical effects of instrument drag were also assessed by comparing the stroke type, stroke frequency and speed of instrumented and uninstrumented dolphins. Data for uninstrumented dolphins were obtained from digital analysis of video recordings taken by a SCUBA diver. For the instrumented dolphin, data were obtained from video recordings as well as from velocity and depth recorders in the instrument package.

Statistics

Linear and curvilinear regressions were determined from least-squares methods using Sigma Plot (Jandel Scientific, 1995). Sigma Stat software (Jandel Scientific, 1995) and Zar (1974) were used for *t*-tests of paired data. Sums-of-squares analyses for curves were calculated using SuperAnova software. Values for significance were set at $P<0.05$. Means are reported ±1 S.E.M.

Results

Swimming gaits of bottlenose dolphins

Similar to previous reports (Videler and Kamermans, 1985; Fish and Hui, 1991), we found that the entire body of the dolphin oscillates as it swims. An undulatory wave progresses behind the dorsal fin down the peduncle to the fluke hinge and finally to the fluke tip (Fig. 1). The dorsal fin moves out of phase with the rostrum and fluke. Maximum upward excursion

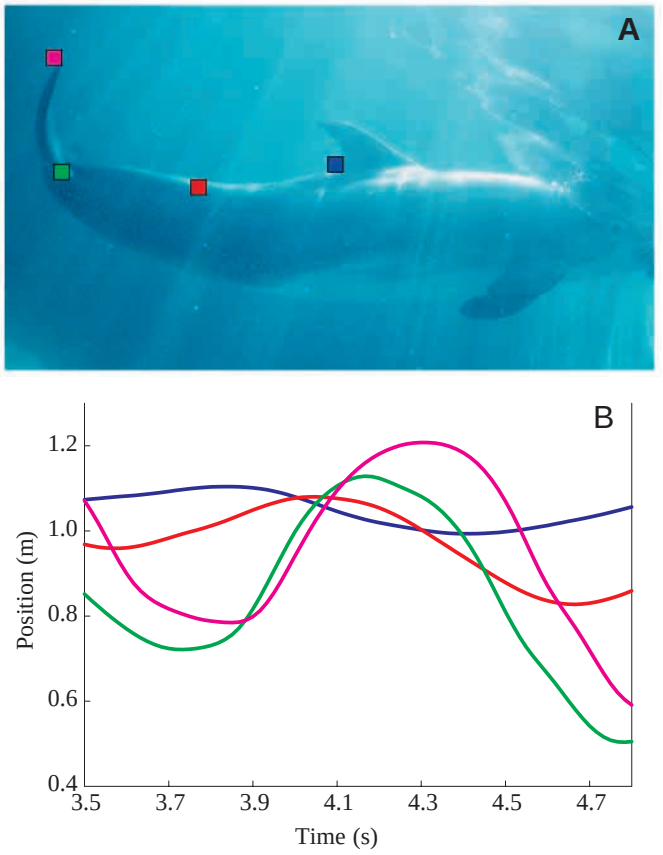

Fig. 1. Video image (A) and range of movement (B) of four anatomical sites during a single stroke for a bottlenose dolphin swimming horizontally next to a boat at 1.5 m s^{-1}. Colored squares in the picture correspond to the line colors illustrating the movements for each site. Note that the dorsal fin (dark blue) reaches its maximum excursion first, followed sequentially by the peduncle (red), the fluke hinge (green) and finally the fluke tip (pink).

of the fluke tip occurs as the dorsal fin is at the bottom of its cycle; the reverse occurs on the downstroke. Each anatomical site differed in range of movement. The amplitude and frequency of these movements were dependent on the speed and power requirements of the animal (Table 2). Both the present study and that of Fish (1993) found no change in fluke amplitude during steady swimming over the range of test speeds. Three different patterns or gaits were observed.

Large-amplitude strokes

The largest stroke amplitudes (representing 20–50 % of body length) occurred at the start of horizontal swims and at the beginning of the descent and ascent phases of dives. The amplitude of these strokes exceeded the range reported for steadily swimming dolphins in an aquarium pool at speeds ranging from 1.2 to 6.0 m s^{-1} (Fish, 1993). The use of this gait corresponded to the periods of greatest acceleration (3.5–4.7 m s^{-2}). The amplitudes for all body segments were larger than those observed during steady swimming. The greatest change in amplitude occurred at the rostrum and was four times that of steady swimming. In comparison, the fluke and dorsal fin regions more than doubled their amplitude during periods of acceleration, while the mid-peduncle region showed the least change (Table 2).

As a result of the methodology, only the movements of the flukes could be recorded during deep dives or horizontal swims at depths exceeding 14 m. Large-amplitude strokes were used during the initial 1–2 s of horizontal swims and initial descents of dives. The period for large-amplitude stroking increased up to 5 s during the initial ascent from 50 and 100 m dives.

Medium-amplitude strokes

Medium-amplitude strokes (approximately 20 % of body length) occurred during steady-state swimming at 1.5–3.7 m s^{-1}. Motion of the head was reduced in comparison with that occurring in association with large-amplitude strokes. The arc of the rostrum covered only 5 % of body length during medium-amplitude stroking. Similarly, the dorsal fin showed comparatively smaller amplitude movements.

There was a significant (P=0.05) increase in the frequency of medium-amplitude strokes with speed during steady swimming over the range 0.6–3.7 m s^{-1} (Fig. 2A). Dolphins

Table 2. *Primary locomotor modes of swimming and diving bottlenose dolphins*

Gait	Use	Duration	Stroke frequency (Hz)	Amplitude (% body length) R:D:F
Large-amplitude	Acceleration	Brief (1–5 s)	>0.43×speed (1.5 to >3 Hz)	20:10:40 Declines rapidly as speed increases
Medium-amplitude	Cruising	Extended (1 s to >1 min)	0.43×speed (0.5–3 Hz)	5:5:20
Glide	Energy conservation	Dependent on dive depth (1–50 s)	0	0:0:0

Stroke frequency increased linearly with speed during steady swimming (see text). During periods of acceleration, stroke frequency was higher than indicated by this relationship.

Relative changes in stroke amplitudes are given for the rostrum (R), dorsal fin (D) and fluke (F) for each gait.

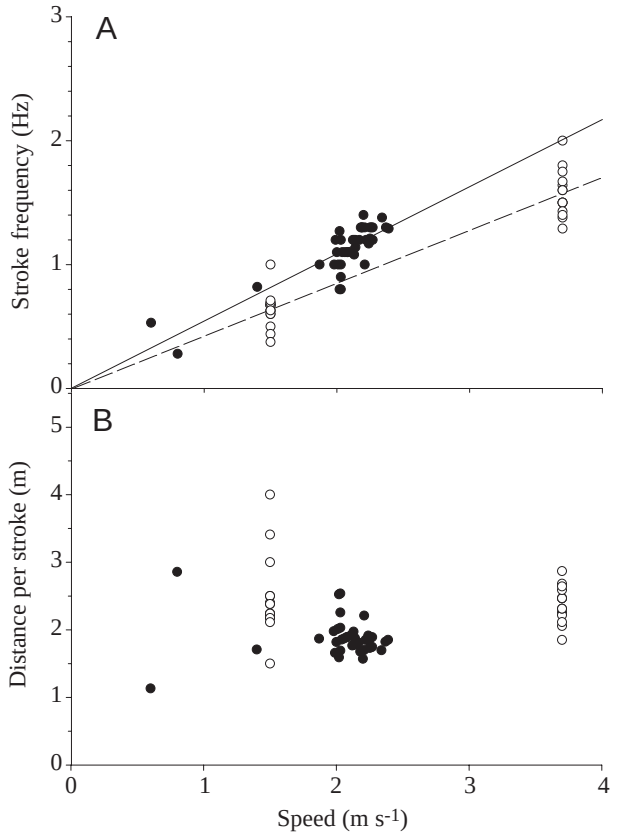

Fig. 2. Stroke frequency (A) and distance traveled per stroke (B) in relation to swimming speed for bottlenose dolphins. Data for instrumented (filled circles) and uninstrumented (open circles) dolphins are compared. Solid and dashed lines denote the least-squares linear regressions through the data points. Regressions for stroke frequency show a significant difference between the instrumented and uninstrumented animals (P<0.05). The distance moved per stroke was independent of speed in both groups of dolphins. Equations for the regression lines are given in the text.

with and without instrumentation showed linear increases in stroke frequency (f) with speed (v), but differed in the magnitude of the response. The regression for uninstrumented dolphins was:

$$f = 0.43v \quad (3)$$

(N=30, r^2=0.90, P<0.05), where stroke frequency is in strokes s^{-1} (Hz) and speed is in m s^{-1}. The stroke frequency of the instrumented dolphin was approximately 27 % higher at comparable speeds to the uninstrumented dolphins and was described by the equation:

$$f = 0.54v \quad (4)$$

(N=41, r^2=0.73, P<0.05). The distance traveled per stroke (Fig. 2B) did not change significantly with speed over the range tested for either the instrumented (r^2=0.008, N=41) or uninstrumented (r^2=0.01, N=30) dolphins. The mean distance per stroke was approximately 0.5 m (27 %) less for the instrumented dolphin than for uninstrumented dolphins swimming at comparable speeds.

Glides

Dolphins incorporated short (3–14 m) and long (>14 m) glide sequences during activity. Short glides occurred at the end of every ascent or descent, as the dolphin came to a stop or changed direction. Ascent glides ranged from 6 to 14 m in distance traveled (mean 9.3±2.5 m, N=28) and showed a mean deceleration of 0.07±0.12 m s^{-2} (N=10). Uninstrumented dolphins also demonstrated short periods of gliding associated with burst-and-glide propulsion during both horizontal submerged swimming and diving. These resulted in brief periods of deceleration before stroking resumed. The instrumented dolphin limited burst-and-glide propulsion to diving periods. We attribute the absence of burst-and-glide activity during horizontal swimming to the added drag of the instrument package. Long-distance gliding was an important component of the descent phase of dives for all dolphins. Glide distance varied with depth as described below.

Variations in gait

In addition to the three distinct gaits described above, dolphins utilized several variations of these patterns. Small-amplitude strokes (<20 % of body length) occurred intermittently as animals made the transition between active swimming and gliding. These smaller strokes also occurred between periods of medium-amplitude stroking. A variety of braking motions that included holding the fluke up, down or to either side were used by dolphins to decelerate.

Locomotor mode during swimming and diving

Horizontal swimming

Horizontal swimming by dolphins near the water surface or submerged at 5–16 m involved similar locomotor modes. For horizontal distances less than 15 m, the dolphins initially accelerated using large-amplitude strokes, followed by a period of decreasing stroke amplitude and finally passive gliding to the end point. The initial acceleration enabled the dolphins to reach speeds of 2.0–3.5 m s^{-1} in less than 2 s. Longer periods of steady-state swimming on the water surface at 1.5–3.7 m s^{-1} were accomplished by medium-amplitude stroking. Glide periods during steady-state swimming rarely exceeded 2 s.

Shallow dives

All shallow dives matched one of the following patterns with minor variation. Dives to 12 m by uninstrumented dolphins began with one or two large-amplitude strokes, resulting in a travel speed of 2.0 m s^{-1}. Starting at a depth of 4–6 m, the animals glided for approximately 5 m before braking or veering into a horizontal glide. Because of the short distance involved, the dolphins were able to glide to the surface after one or two medium-amplitude strokes at the start of the ascent. Dives to 16 m by the instrumented dolphin also began with a short period of active stroking followed by a short glide. The dolphin actively swam downwards for 9.0±1.9 m (N=10) before gliding the remaining 7.1±1.9 m (N=10). After braking, the dolphin used large-amplitude strokes to begin the ascent. Medium-amplitude strokes were used throughout the mid portion of the

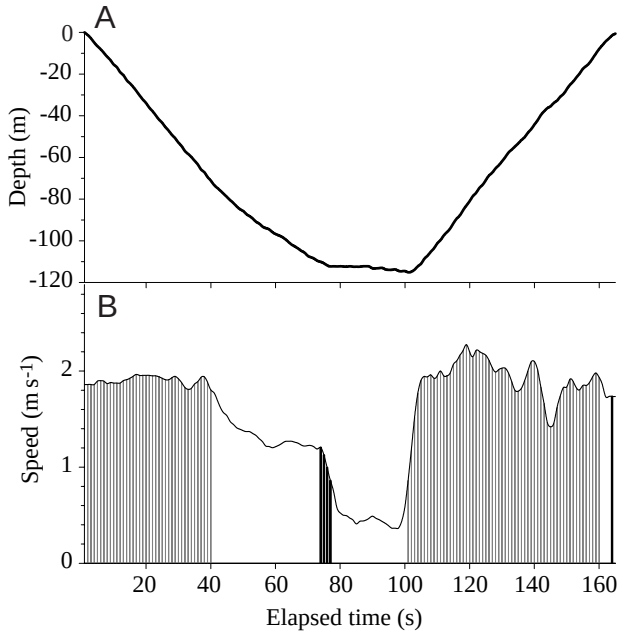

Fig. 3. Representative changes in depth (A) and speed and stroke pattern (B) in relation to dive time for an instrumented dolphin. Maximum dive depth was 112 m. Grey bars denote periods of stroking in which glide periods were less than 1 s in duration. Open areas show periods of continuous gliding or stationing. Black bars indicate braking at the end of the descent and ascent. Note the change in deceleration at 60 s midway through the gliding decent.

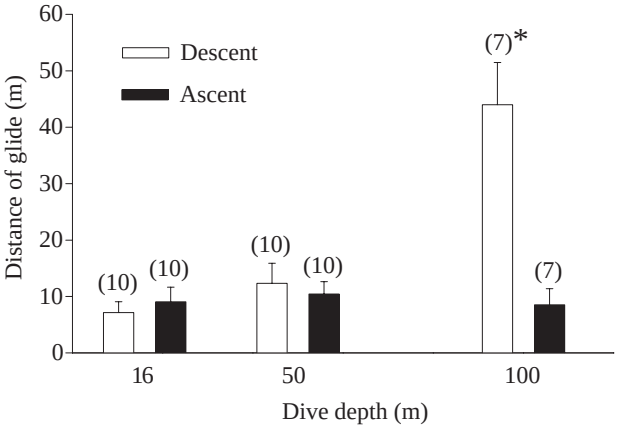

Fig. 4. Glide distance during descent (open columns) and ascent (filled columns) segments of dives in relation to depth for bottlenose dolphins. The height of the columns and lines shows the mean value +1 S.E.M. Numbers in parentheses indicate the total number of dives examined. An asterisk indicates a significant difference between the descent and ascent values for 100 m dives. Glide distances were not significantly different (at $P<0.05$) between ascent and descents for dives ranging from 16 to 50 m. In contrast, significant differences (at $P<0.001$) were found between glide distances for the descent and ascent segments of the 100 m dives.

ascent. As the dolphins approached the surface, stroke amplitude decreased to zero, with the dolphin gliding the remaining 9.1±2.6 m (N=10).

Deep dives

The instrumented dolphin performed ten dives to depths of 50 m and eight dives to depths of 100–112 m. As observed for shallow dives, the dolphin used large-amplitude strokes to begin the descent, followed by medium-amplitude stroking. Intermittent stroking patterns incorporating short periods of gliding between active stroking often occurred during deep dives (Fig. 3). These periods of intermittent propulsion were characteristic for descents and ascents of deep dives but were not observed for shallow dives.

The percentage of time spent gliding during descent changed with depth for the diving dolphins. During 50 m dives, the dolphin glided for 30.3±2.8 % (N=10) of the descent. This increased significantly (at $P<0.001$) to 51.2±3.3 % (N=8) during the 100–112 m dives.

Glide distance for the 50 m dives, 12.3±3.6 m (N=10), was not significantly different (at P=0.21) from the average for 16 m dives. However, glide distance during the descent increased significantly (P=0.01) with dive depths greater than 50 m. The total length of the glide was 43.6±7.0 m (N=8) during 100–112 m dives (Fig. 4). Glides occurring during the ascent showed no significant changes with depth (P=0.27).

The speed of the dolphins during diving was correlated with gliding or stroking periods. An example is shown in Fig. 3. During stroking on the descent of a 112 m dive, the speed of the dolphin was approximately 1.9 m s^{-1}. Cessation of stroking resulted in a period of deceleration that was followed by a constant speed of 1.2 m s^{-1} during the remainder of the descending glide. Speed during the ascent was more variable and corresponded with burst-and-glide activity (Fig. 3).

As with shallower dives, a braking motion occurred at the end of descent, followed by large-amplitude strokes at the beginning of ascent. Average glide distance to the surface was 10.4±2.2 m (N=10) on 50 m dives and 8.5±2.9 m (N=8) on 100–112 m dives.

Drag and buoyant forces

The drag of the dolphins increased significantly with speed and was comparatively higher for the instrumented dolphin (Fig. 5). The least-squares curvilinear regression for the instrumented dolphin was:

$$D = 1.78 + 8.93v^{2.99} \quad (5)$$

(r^2=0.64, P=0.220, N=6). The regression for uninstrumented dolphins was:

$$D = 4.15v^{2.00} \quad (6)$$

(r^2=0.65, P=0.097, N=5), where drag (D) is in newtons and speed (v) is in m s^{-1} for both equations.

For deep-diving dolphins, measured deceleration during gliding changed with depth because of changes in buoyant force. For example, the mean depth during prolonged (>2 s) descending glides was 67.5±23.0 m, with a glide speed of 1.5±0.3 m s^{-1} and a mean deceleration of 0.03±0.06 m s^{-2}

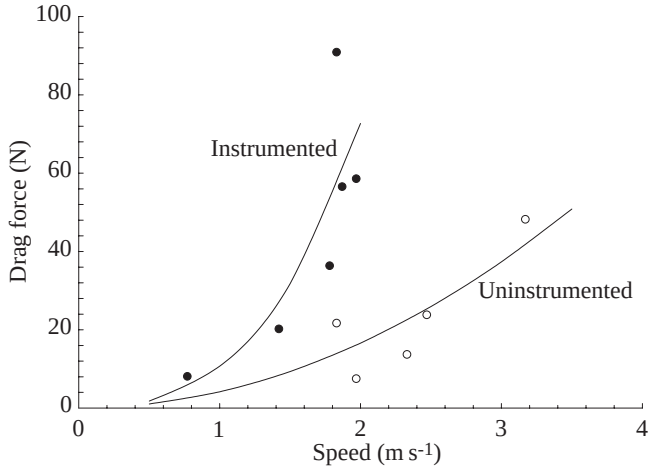

Fig. 5. Body drag in relation to horizontal glide speed for instrumented (filled circles) and uninstrumented (open circles) bottlenose dolphins. Solid lines denote the least-squares curvilinear relationships through the data points. All glide sequences took place at depths greater than three body diameters below the water surface to avoid surface wave effects. Speed represents the mean speed during each glide sequence. Equations for the relationships are given in the text.

(N=27 glide sequences). The decelerating force acting on vertically diving dolphins, calculated from the product of deceleration (0.03 m s^{-2}) and the mass of the instrumented dolphin including entrained water (202 kg), was 6.1 N. This compares with a drag of 31.8 N for gliding dolphins moving horizontally at the same speed (Fig. 5; equation 5). Presumably, the drag of the vertically diving dolphin was countered by a downward force of 25.7 N (31.8–25.7=6.1) (Table 3). Similar calculations for the ascent phase demonstrate the positive effect of buoyancy as a dolphin nears the water surface. The mean depth of gliding for ascent from instrumented dives was 5.5±2.2 m, with a mean speed of 1.6±0.2 m s^{-1} and deceleration of 0.07±0.12 m s^{-2} (N=10). The product of deceleration and mass is 14.1 N for the dolphins on a vertical ascent. In comparison, the calculated drag for horizontally gliding dolphins moving at 1.6 m s^{-1} is 38.4 N (equation 5). Thus, the final ascent drag was countered by an upward buoyant force of 24.3 N (38.4–24.3=14.1).

From these calculations, we find that the buoyant force acting on the diving dolphins in this study changed from +24.3 N near the water surface (5.5 m depth) to –25.7 N at a depth of 67.5 m, a difference of 50.0 N. This is equivalent to a change in water displacement of 5.1 l (50.0 N/9.8 m s^{-2}=5.1 kg or approximately 5.1 l of water). Such a change in displacement is reasonable since dolphins dive following inspiration and air compresses with depth. From equation 1, an initial lung volume of 8–10 l would be needed to achieve this magnitude of volume change in the diving dolphin, which is within the reported range for a 177 kg dolphin (Ridgway et al., 1969; Stahl, 1967).

Fig. 6 illustrates the changes in buoyant force of 8.5 l of air with depth for diving dolphins. This curve and the calculated buoyancy of the dolphin differed consistently by 33.2 N, and we assume that this was due to the weight of the dolphin's body. Thus, for the instrumented dolphin, diving with a lung volume of 8.5 l, equation 2 becomes:

$$B_D = 83/(1 + 0.1h) - 33.2\,, \qquad (7)$$

where B_D is the buoyant force in newtons at depth h in m, 83 N is the buoyant force of 8.5 l of air and –33.2 N is the buoyancy of the dolphin's body without air. The net force acting on the gliding dolphin can then be calculated from the difference between this buoyant force and total body drag (Fig. 5).

The above calculations are appropriate for gliding dolphins in which swimming motions are absent. To calculate the drag on swimming dolphins, we need to account for the additional drag due to locomotor movements. A conservative estimate of this active drag is three times that of the gliding animal (Lighthill, 1975, 1971; Webb, 1975, 1984; Williams and Kooyman, 1985; Fish, 1993).

Table 3. *Locomotor variables, total body drag and buoyant forces for a bottlenose dolphin during a 100 m dive*

	Deceleration (m s^{-2})	Speed (m s^{-1})	Net force (N)	Drag (N)	Buoyancy (N)	Depth (m)
Descent glide	0.03±0.06 (27)	1.5±0.3 (27)	6.1	31.8	–25.7	67.5
Ascent glide	0.07±0.12 (10)	1.6±0.2 (10)	–14.1	–38.4	24.3	5.5
Descent swimming		1.7±0.0	160.6	136.3	24.3	5.5
Ascent swimming		1.9±0.0	–213.6	–187.9	–25.7	67.5

Gliding and swimming during ascent and descent are compared.

Deceleration, speed and depth were measured for a dolphin wearing an instrument pack.

Net force, drag and buoyancy were calculated as described in the text. Drag calculations for swimming on ascent and descent include an active drag factor of 3 (Fish, 1993; Lighthill, 1971, 1975; Webb, 1975, 1984) to account for the additional drag associated with swimming movements.

All downward forces relative to the water surface are indicated by a negative sign.

Numbers in parentheses indicate N for the measured variables.

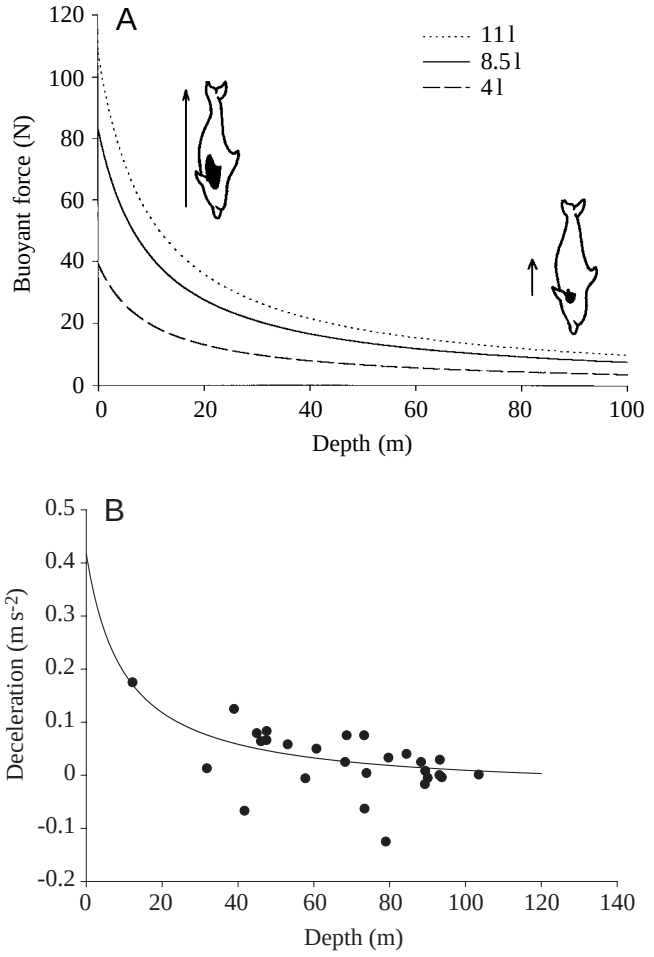

Fig. 6. Changes in the buoyant force of lung air (A) and deceleration (B) in relation to dive depth in bottlenose dolphins. Calculations for buoyant force are based on equations presented in the text and are compared for three different initial lung volumes. Note the rapid decline in buoyant force with depth as the water pressure progressively collapses the lungs. The decline in deceleration of gliding dolphins (B) determined from video analyses paralleled that calculated for buoyant force. Each point represents an individual glide sequence. The solid line in B is not a regression for the data, but rather the calculated deceleration based on buoyancy changes with depth (see text).

Effects of instrumentation

Average speeds during diving and horizontal swimming were 9–10 % lower for the instrumented dolphin than for uninstrumented dolphins. Drag was 3.3 times higher for the instrumented dolphin at the mean gliding speed of 1.47 m s^{-1} (Fig. 5). The elevated drag resulted in a 27 % reduction in distance achieved per stroke and a concomitant increase in stroke frequency (Fig. 2). Although stroke amplitude appeared to be higher for the instrumented dolphin, differences in measurement techniques for instrumented and uninstrumented animals prevented accurate comparisons. Because of the demonstrated effects of the instrumentation on drag and swimming mechanics, the glide distances reported here should be considered as conservative estimates of the true performance of uninstrumented dolphins performing deep dives.

Discussion

The importance of gait transitions during swimming and diving

Foraging aquatic mammals must divide their time between two important resources, oxygen located at the water surface and prey items located at depth (Dunstone and O'Connor, 1979). The swimming modes selected by mammals moving between these resources will affect their locomotor efficiency and, ultimately, the cost/benefit relationships for foraging. Previous studies with dolphins have shown that elevating swimming speeds during ascent and descent to decrease the duration of a dive leads to an extraordinarily rapid depletion of limited oxygen reserves (Williams et al., 1993). Travel too slowly, however, and time becomes limiting as basal metabolic demands exhaust the available oxygen (Williams et al., 1999).

Data from the present study demonstrate that bottlenose dolphins tailor their swimming patterns to diving depth, a strategy that leads to energetic efficiency (Figs 3, 4). As found for running animals (Heglund et al., 1974; Taylor, 1978; Hoyt and Taylor, 1981), changes in gait by swimming and diving dolphins were associated with specific tasks and speeds (Table 2; Fig. 3). Dolphins switched gaits primarily in conjunction with acceleration needs. During initial acceleration from rest, stroke frequencies and fluke amplitudes often exceeded those used during steady swimming. Large-amplitude movements of the head and back accompanied these large fluke motions. The tip of the rostrum showed an excursion of nearly 20 % of body length, while fluke amplitude exceeded 40 % of body length (Table 2). As the dolphin's speed increased, stroke amplitude gradually decreased to the values observed during steady-state swimming. These results are consistent with models that predict increased mechanical efficiency during low-speed swimming when thrust is produced by accelerating a large mass of fluid (per time) to a low velocity instead of accelerating a small mass to a high velocity (Alexander, 1977).

During diving, dolphins minimized the use of large-amplitude strokes and incorporated prolonged glide periods as speed and coincident drag increased. Large-amplitude strokes only occurred for brief (<5 s) periods during the initial descent and ascent. Except for these initial periods, diving dolphins relied on medium-amplitude strokes and, when possible, even smaller stroking movements. The smaller-amplitude strokes occurred during transitions between steady-state stroking and gliding, with stroke frequency remaining unchanged. These results are not surprising when the hydrodynamics are considered. High-amplitude movements are a departure from the streamlined shape of the dolphin and theoretically result in elevated levels of drag, especially as stroke amplitude is increased (Fish et al., 1988; Lighthill, 1971; Webb, 1975). An actively swimming animal may encounter a three- to fivefold increase in total body drag over gliding values as a result of

elevated pressure drag (Fish et al., 1988), separation or thinning of the boundary layer (Lighthill, 1971) and increased drag from thrust production (Webb, 1975). The marked effect of even small adjustments in posture on drag and forward movement of the dolphin was observed when an animal used braking movements to reduce speed. Raising the fluke a distance equivalent to 10 % of body length resulted in an 11.5-fold increase in total body drag.

Although prolonged gliding allows diving dolphins to avoid active drag, it places a limit on maintaining propulsion. To circumvent this, dolphins and other swimmers often rely on a burst-and-glide style of swimming that incorporates short periods of stroking during prolonged glide sequences to maintain forward speed (Videler, 1981; Videler and Weihs, 1982; Weihs, 1974). Despite elevated drag associated with re-acceleration between glides, the calculated energetic cost for this interrupted mode of swimming is significantly lower than for continuous swimming (Blake, 1983).

Because dolphins produce power by oscillating their flukes (Lang and Daybell, 1963; Slijper, 1961; Videler and Kamermans, 1985), the mass of the fluke plus entrained water must be decelerated to a stop then re-accelerated in the opposite direction both at the top and bottom of each stroke. The alternate storage and release of elastic energy in conjunction with fluke movements could serve as a potential energy-conserving mechanism. Changes in the axial body of the swimming dolphin are qualitatively similar to those of galloping terrestrial mammals in which the trunk is used as a spring to store elastic energy (Taylor, 1978). Several spring-like tissues have been implicated as energy-saving mechanisms for swimming dolphins. Pabst (1990) described a crossed, helically wound, fiber array encasing the dolphin body. The fiber array, derived from ligaments, muscle tendons and blubber tissue, gains rigidity because of the tension it is under. This array may act as a spring, storing energy during part of the stroke cycle and recovering it during the remainder (Pabst, 1990). Although intriguing, such elastic storage mechanisms have yet to be tested in a freely swimming dolphin and warrant further investigation.

The swimming mechanics of dolphins share other features common to terrestrial animals and swimming humans. In terrestrial mammals, stride frequency increases linearly with speed during walking and trotting. As speed increases, many runners switch to a gallop in which speed is achieved by lengthening the stride rather than by increasing stride frequency (Heglund et al., 1974). Conversely, human swimmers decrease the distance per stroke (the aquatic equivalent of stride length) and increase the stroke frequency to achieve greater speeds (Costill et al., 1991). Horizontally swimming dolphins combine both patterns and increase stroke frequency linearly with speed while the distance per stroke remains relatively constant (Fig. 2). Mean distance per stroke was 2.4 m irrespective of speed. Stroke amplitude in dolphins also remained constant during horizontal swimming, with amplitude remaining at 20 % of body length for steady speeds ranging from 1.2 to 6.0 m s^{-1} (Table 2; Fish, 1993).

Buoyancy, gliding and energy expenditure during diving

Locomotor performance by horizontally swimming and vertically diving dolphins is influenced by very different physical factors. During horizontal swimming near the water surface, dolphins encounter high levels of drag associated with wave generation (Hertel, 1969). The effects of wave drag are negligible for diving dolphins once the animal is three body diameters below the water surface. Diving dolphins, however, face unique changes in buoyant forces with depth that become a major influence on performance and behavior.

An interesting finding in this study was the use of prolonged periods of gliding by dolphins for dives exceeding a depth of 50 m. Approximately 50 % of the descent phase was spent gliding rather than actively swimming on dives to a depth of 100 m. Deceleration rate decreased progressively during prolonged glides, finally reaching a point of zero deceleration at a depth of 90 m (Fig. 6B). These extended glides occurred only during the descent phase of deep dives (Fig. 4), suggesting that physical factors rather than distance *per se* dictated glide performance. Changes in buoyancy with depth due to lung compression from increased pressure probably contributed to these results. In general, dolphins dive after inspiration and exhale upon surfacing, indicating that they dive with inflated lungs (Ridgway et al., 1969; present study). Goforth (1986) reported that the diving lung volume of dolphins was approximately 75 % of maximum lung volume. The bronchi and trachea as well as the alveoli of the cetacean lung are collapsible, as determined in pressure chamber tests. Only the bony nares, with a volume of 50 ml, are rigid (Ridgway et al., 1969). Such a morphological structure permits a progressive collapse of the thorax with increased pressure at depth.

Compression of the air spaces in dolphins decreases volume without an accompanying reduction in mass. As a result, the dolphin becomes less buoyant with depth. Although it was not possible to measure directly the volume of air in an actively diving dolphin, the range of lung volumes and their effect on buoyancy have been determined for excised lungs from a 200 kg bottlenose dolphin (Ridgway et al., 1969). Ridgway and Howard (1979) calculated that alveolar collapse is complete once bottlenose dolphins experience pressures equivalent to 65–70 m in depth. The theoretical changes in buoyant force associated with this collapse are shown in Fig. 6. The maximum respiratory volume of the dolphin (11 l) was associated with neutral to slightly buoyant forces at full inflation and with a negative buoyancy of 10 kg when the lungs were deflated. In the present study, we found that changes in the deceleration rate of gliding dolphins were similar in pattern to the calculated changes in buoyant forces with lung compression (Fig. 6), suggesting a correlation between pressure and locomotor movements at depth.

Using this basic information, we can examine the relationship between physical factors and the swimming behavior of dolphins during diving. Major physical forces include buoyancy, acting in an upward or downward direction depending on diving depth, and drag opposing the forward

Table 4. *Calculated energetic costs for overcoming drag and buoyancy during a 100 m dive by an adult bottlenose dolphin*

	Active swim distance (m)		Speed ($m\,s^{-1}$)		Locomotor cost (J)
	Descent	Ascent	Descent	Ascent	Total
Measured	53	92	1.73	1.90	26 064
Neutral buoyancy					
Total time-fixed	95	95	1.76	1.76	28 608
Speed-fixed	95	95	1.73	1.90	31 465

Locomotor costs were determined from the product of net forces (Table 3) and distance traveled.

Measured values for a dolphin wearing an instrument package are compared with those for two models assuming neutral buoyancy. The time-fixed model maintains the total dive time to that measured for the diving dolphin. Swimming speed is adjusted to accommodate the time requirement. The speed-fixed model maintains the swimming speeds for ascent and descent to those measured for the diving dolphin. However, the duration of the dive is adjusted to accommodate the neutral buoyancy and speed requirements.

movement of the dolphin. For the straight-line trained dives in the present study, total body drag acts upwards as the animal descends and downwards relative to the motion of the dolphin during ascent. The combined effects of these forces during various segments of a 100 m dive by a bottlenose dolphin are presented in Table 3. For the instrumented dolphin, passive gliding predominated when the calculated net force opposing the animal was less than 21 N. If the opposing force was higher, prolonged gliding was untenable and the dolphin switched to either stroking or short periods of burst-and-glide swimming. This may explain in part the high proportion of gliding during vertical diving in comparison with horizontal swimming by the same animal. With no buoyancy advantage during horizontal swims, the calculated drag for the speed range examined exceeded 21 N, and little gliding occurred. As mentioned above, descending glides during long descents reached zero deceleration at depth of approximately 90 m depth. At this depth, the downward force imparted by negative buoyancy fully counteracted the calculated drag and provided the dolphin with a theoretical ‘free ride’.

Although the progressive negative buoyancy with depth provides a locomotor advantage during descent, the reverse occurs during ascent. The same force that pulled the dolphin down must be overcome for the animal to return to the surface, seemingly negating any benefit. If energetic and hydrodynamic factors are considered together, we find that gliding provides an overall advantage for the diver. This is due to a significant reduction in active drag, which contributes to the energetic efficiency of burst-and-glide swimming (Blake, 1983). The locomotor behavior of diving dolphins is analogous to a type of burst-and-glide swimming, with exceptionally long glides facilitated by changes in buoyancy with depth.

The energetic advantage of gliding may be determined theoretically by calculating the total energy expended to overcome drag and buoyancy (locomotor cost) in diving dolphins. We estimated locomotor costs from the product of the net forces and mean distance covered during gliding and swimming (Tables 3, 4). On the basis of the straight-line dives examined in this study, the locomotor cost for an instrumented dolphin performing a 100 m dive was 26 064 J ($0.74\,J\,kg^{-1}\,m^{-1}$). This compares with a minimum locomotor cost of $0.73\,J\,kg^{-1}\,m^{-1}$ calculated from the difference between maintenance costs and total minimum cost of transport for bottlenose dolphins swimming near the water surface (Williams et al., 1992; Williams, 1999). In view of the similarity in locomotor costs between these swimmers and divers, it is apparent that deep-diving dolphins select energetically efficient modes of locomotion. Despite the effect of the instrumentation (Figs 2, 5), the diving dolphins in the present study were able to match the predicted minimum locomotor costs of swimming dolphins by taking advantage of changes in buoyancy. The theoretical costs are considerably higher if we assume that dolphins are neutrally buoyant throughout the dive. If a dolphin were neutrally buoyant and tried to maintain the same dive duration for a 100 m dive, as measured in this study, then locomotor costs would increase by 10 %. A neutrally buoyant dolphin maintaining the same swimming speeds (with a consequent shorter dive duration) for a 100 m dive experiences a 21 % increase in energetic requirements (Table 4).

The reduction in active drag during gliding was the primary factor leading to the energetic savings during diving rather than changes in buoyancy *per se*. Because of the marked influence of the instrument package on body drag (Fig. 5), these calculations admittedly represent a conservative estimate of the effects of buoyancy on gliding performance. It is likely that uninstrumented dolphins will exhibit even greater gliding performance with potentially greater energetic savings than indicated in these calculations. The reduction in power requirements and hence energetic costs associated with gliding initially appears modest. However, the savings may provide a significant advantage to free-ranging dolphins by allowing extended foraging time through the conservation of limited energy stores.

In conclusion, the present study illustrates how the interrelationships between swimming mechanics, buoyancy and underwater behavior support energetically efficient locomotion in diving dolphins. Similar conclusions regarding buoyancy and performance have been reached for other marine animals, including free-ranging elephant seals (*Mirounga augustirostris*) (Webb et al., 1998), diving ducks (Lovvorn et al., 1991) and a variety of fish species (Alexander, 1990). Variation in glide performance facilitated by changes in buoyancy appears to be an important mechanism that enables marine mammals to conserve limited oxygen stores during submergence. A corollary to this study suggests that speed alone is a relatively poor indicator of aquatic effort and may be inadequate for assessing energetic costs in diving marine mammals. Both gliding and active swimming often occur at similar speeds. However, the energetic consequences of each may be very different.

This series of papers on the diving physiology of dolphins was inspired by the work of Gerald L. Kooyman; they are dedicated to him in celebration of his remarkable research career and influence on all comparative physiologists. This study was supported by an Office of Naval Research grant and ASSEE fellowship (N00014-95-1-1023) to T.M.W. The authors thank the many people that assisted in this study including the trainers and dolphins at the SPAWAR facility in San Diego and the Dolphin Experience in the Bahamas. Computer assistance by S. Collier at Texas A&M University is gratefully acknowledged. In addition, the authors appreciate the critical evaluation of this manuscript by S. Noren, D. Noren and S. Kohin and lively discussions with F. Fish. All experimental procedures were evaluated and approved according to animal welfare regulations specified by NIH guidelines. UCSC and SPAWAR Systems Center (San Diego) conducted institutional animal use reviews.

References

Abrahams, M. V. and Colgan, P. W. (1985). Risk of predation, hydrodynamic efficiency and their influence on school structure. *Env. Biol. Fish.* **13**, 195–202.

Alexander, R. McN. (1977). Swimming. In *Mechanics and Energetics of Animal Locomotion* (ed. R. McN. Alexander and G. Goldspink), pp. 222–247. London: Chapman & Hall, Halsted Press Book.

Alexander, R. McN. (1990). Size, speed and buoyancy in aquatic animals. *Am. Zool.* **30**, 189–196.

Belyayev, V. V. and Zuyev, G. V. (1969). Hydrodynamic hypothesis of schooling in fishes. *J. Ichthyol.* **9**, 578–584.

Blake, R. W. (1983). *Fish Locomotion*. Cambridge: Cambridge University Press. 208pp.

Boyd, I. L., McCafferty, D. J. and Walker, T. R. (1997). Variation in foraging effort by lactating Antarctic fur seals: response to simulated increased foraging costs. *Behav. Ecol. Sociobiol.* **40**, 135–144.

Breder, C. M., Jr (1965). Vortices and fish schools. *Zoologica* **50**, 97–114.

Castellini, M. A. (1985). Closed systems: Resolving potentially conflicting demands of diving and exercise in marine mammals. In *Circulation, Respiration and Metabolism* (ed. R. Gilles), pp. 219–226. Berlin: Springer-Verlag.

Castellini, M. A., Murphy, B. J., Fedak, M. A., Ronald, K., Gofton, N. and Hochachka, P. W. (1985). Potentially conflicting metabolic demands of diving and exercise in seals. *J. Appl. Physiol.* **58**, 392–399.

Costill, D. L., Maglischo, E. W. and Richardson, A. B. (1991). Swimming. In *Handbook of Sports Medicine and Science*, pp. 176–177. London: Blackwell Science Inc.

Daniel, T. L. (1984). Unsteady aspects of aquatic locomotion. *Am. Zool.* **24**, 121–134.

Davis, R. W., Collier, S. O., Hagey, W., Williams, T. M. and LeBoeuf, B. J. (1999). A video system and three dimensional dive recorder for marine mammals: Using video and virtual reality to study diving behavior. *Proceedings of the Fifth European Conference on Biotelemetry, Strasbourg, France*.

Dunstone, N. and O'Connor, R. J. (1979). Optimal foraging in an amphibious mammal. I. The aqualung effect. *Anim. Behav.* **27**, 1182–1194.

Fish, F. E. (1992). Aquatic locomotion. In *Mammalian Energetics: Interdisciplinary Views of Metabolism and Reproduction* (ed. T. Tomasi and T. Horton). Ithaca, NY: Comstock Publ. Ass. 276pp.

Fish, F. E. (1993). Power output and propulsive efficiency of swimming bottlenose dolphins (*Tursiops truncatus*). *J. Exp. Biol.* **185**, 179–183.

Fish, F. E., Fegely, J. F. and Xanthopoulos, C. J. (1991). Burst-and-coast swimming in schooling fish (*Notemigonus crysoleucas*) with implications for energy economy. *Comp. Biochem. Physiol.* **100**A, 633–637.

Fish, F. and Hui, C. (1991). Dolphin swimming – a review. *Mammal Rev.* **21**, 181–195.

Fish, F. E., Innes, S. and Ronald, K. (1988). Kinematics and estimated thrust production of swimming harp and ringed seals. *J. Exp. Biol.* **137**, 157–173.

Giancoli, D. C. (1984). *General Physics* (ed. L. Mihatov). Englewood Cliffs, NJ: Prentice-Hall Inc. 892pp.

Goforth, H. W. (1986). Glycogenolytic responses and force production characteristics of a bottlenose dolphin (*Tursiops truncatus*), while exercising against a force transducer. PhD dissertation, University of California, Los Angeles, USA.

Heglund, N. C., Taylor, C. R. and McMahon, T. A. (1974). Scaling stride frequency and gait to animal size: mice to horses. *Science* **186**, 1112–1113.

Heine, J. N. (1995). *Mastering Advanced Diving*. Third edition. St Louis, MO: Mosby-Year Book, Inc. 293pp.

Hertel, H. (1969). Hydrodynamics of swimming and wave-riding dolphins. In *The Biology of Marine Mammals* (ed. H. T. Andersen), pp. 31–63. New York: Academic Press, Inc.

Hoyt, D. F. and Taylor, C. R. (1981). Gait and the energetics of locomotion in horses. *Nature* **292**, 239–240.

Hui, C. A. (1987). Power and speed of swimming dolphins. *J. Mammal.* **68**, 126–132.

Lang, T. G. (1974). Speed, power and drag measurements of dolphins and porpoises. In *Swimming and Flying in Nature*, vol. 2 (ed. T. Y. Wu, C. J. Brokaw and C. Brennen), pp. 553–572. New York: Plenum Press.

Lang, T. G. and Daybell, D. A. (1963). Porpoise performance tests in a seawater tank. In *NOTS Technical Publication 3063.* NAVWEPS Report 8060, Naval Ordinance Test Station, China Lake.

Lang, T. G. and Norris, K. S. (1966). Swimming speed of a Pacific bottlenose dolphin. *Science* **151**, 588–590.

Lighthill, M. J. (1971). Large-amplitude elongated-body theory of fish locomotion. *Proc. R. Soc. Lond. B* **179**, 125–138.

Lighthill, M. J. (1975). *Mathematical Biofluid Dynamics*. Philadelphia: Society for Industrial and Applied Mathematics.

Lovvorn, J. R., Jones, D. R. and Blake, R. W. (1991). Mechanics of underwater locomotion in diving ducks: drag, buoyancy and acceleration in a size gradient of species. *J. Exp. Biol.* **159**, 89–108.

Magana, S. A., Hoyt, D. F., Wickler, S. J., Lewis, C. C., Garcia, S. B. and Padilla, O. R. (1997). The effect of load carrying on preferred trotting speed in horses. *Am. Zool.* **37**, 176a.

Pabst, A. D. (1990). Axial muscles and connective tissues of the bottlenose dolphin. In *The Bottlenose Dolphin* (ed. S. Leatherwood and R. R. Reeves), pp. 51–67. San Diego, CA: Academic Press, Inc.

Ridgway, S. H. and Howard, R. (1979). Dolphin lung collapse and intramuscular circulation during free diving: Evidence from nitrogen washout. *Science* **206**, 1182–1183.

Ridgway, S. H., Scronce, B. L. and Kanwisher, J. (1969).

Respiration and deep diving in the bottlenose porpoise. *Science* **166**, 1651–1654.

Rohr, J., Latz, M. I., Fallon, S., Nauen, J. C. and Hendricks, E. (1998). Experimental approaches towards interpreting dolphin-simulated bioluminescence. *J. Exp. Biol.* **201**, 1447–1460.

Slijper, E. J. (1961). Locomotion and locomotory organs in whales and dolphins (Cetacea). *Symp. Zool. Soc. Lond.* **5**, 77–94.

Stahl, W. R. (1967). Scaling respiratory variables in mammals. *J. Appl. Physiol.* **22**, 453–460.

Taylor, C. R. (1978). Why change gaits? Recruitment of muscles and muscle fibers as a function of speed and gait. *Am. Zool.* **18**, 153–161.

Videler, J. J. (1981). Swimming movements, body structure and propulsion in cod (*Gadus morhua*). In *Vertebrate Locomotion*, vol. 48 (ed. M. H. Day), pp. 1–27. London: Academic Press.

Videler, J. J. and Kamermans, P. (1985). Differences between upstroke and downstroke in swimming dolphins. *J. Exp. Biol.* **119**, 265–274.

Videler, J. J. and Weihs, D. (1982). Energetic advantages of burst-and-coast swimming of fish at high speeds. *J. Exp. Biol.* **97**, 169–178.

Vogel, S. (1981). *Life in Moving Fluids*. Boston: Willard Grant Press. 352pp.

Webb, P. M., Crocker, D. E., Blackwell, S. B., Costa, D. P. and LeBoeuf, B. J. (1998). Effects of buoyancy on the diving behavior of northern elephant seals. *J. Exp. Biol.* **201**, 2349–2358.

Webb, P. W. (1975). Hydrodynamics and energetics of fish propulsion. *Bull. Fish. Res. Bd Can.* **190**, 1–158.

Webb, P. W. (1984). Body form, locomotion and foraging in aquatic vertebrates. *Am. Zool.* **24**, 107–120.

Weihs, D. (1973). Hydromechanics of fish schooling. *Nature* **241**, 290–291.

Weihs, D. (1974). Energetic advantages of burst swimming of fish. *J. Theor. Biol.* **48**, 215–229.

Williams, T. M. (1983). Locomotion in the North American mink, a semi-aquatic mammal. II. The effect of an elongate body on running energetics and gait pattern. *J. Exp. Biol.* **105**, 283–295.

Williams, T. M. (1996). Strategies for reducing foraging costs in dolphins. In *Aquatic Predators and their Prey* (ed. S. P. R. Greenstreet and M. L. Tasker), pp. 4–9. Cambridge: Blackwell Scientific Publications, Oxford.

Williams, T. M. (1999). The evolution of cost efficient swimming in marine mammals: limits to energetic optimization. *Phil. Trans. R. Soc. Lond. B* **354**, 193–201.

Williams, T. M., Friedl, W. A., Fong, M. L., Yamada, R. M., Sedivy, P. and Haun, J. E. (1992). Travel at low energetic cost by swimming and wave-riding bottlenose dolphins. *Nature* **355**, 821–823.

Williams, T. M., Friedl, W. A., Haun, J. E. and Chun, N. K. (1993). Balancing power and speed in bottlenose dolphins (*Tursiops truncatus*). In *Marine Mammals: Advances in Behavioural and Population Biology*, vol. 66 (ed. I. L. Boyd) pp. 383–394. Oxford: Clarendon Press.

Williams, T. M. , Haun, J. E. and Friedl, W. A. (1999). The diving physiology of bottlenose dolphins (*Tursiops truncatus*). I. Balancing the demands of exercise for energy conservation at depth. *J. Exp. Biol.* **202**, 2763–2769.

Williams, T. M. and Kooyman, G. L. (1985). Swimming performance and hydrodynamic characteristics of harbor seals (*Phoca vitulina*). *Physiol. Zool.* **58**, 576–589.

Wilson, R. P., Grant, W. S. and Duffy, D. S. (1986). Recording devices on free-ranging marine animals: does measurement affect foraging performance? *Ecology* **67**, 1091–1093.

Würsig, B. and Würsig, M. (1979). Behavior and ecology of the bottlenose dolphin, *Tursiops truncatus*, in the south Atlantic. *Fish. Bull.* **77**, 399–412.

Zar, J. H. (1974). *Biostatistical Analysis*. Englewood Cliffs, NJ: Prentice Hall, Inc. 620pp.